

## Tyr Phosphatase–Mediated P-ERK Inhibition Suppresses Senescence in EIA + *v-raf* Transformed Cells, Which, Paradoxically, Are Apoptosis-Protected in a MEK-Dependent Manner<sup>1,2</sup>

Stefania De Vitis<sup>\*,3</sup>, Antonella Sonia Treglia<sup>\*,3</sup>, Luca Ulianich<sup>†</sup>, Stefano Turco<sup>\*</sup>, Giuseppe Terrazzano<sup>‡,§</sup>, Angela Lombardi<sup>\*,‡</sup>, Claudia Miele<sup>\*,‡</sup>, Corrado Garbi<sup>‡</sup>, Francesco Beguinot<sup>\*,‡</sup> and Bruno Di Jeso<sup>\*</sup>

\*Dipartimento di Scienze e Tecnologie Biologiche ed Ambientali, Facoltà di Scienze Matematiche Fisiche e Naturali, Università degli Studi del Salento, Lecce, Italy; <sup>†</sup>Dipartimento di Biologia e Patologia Cellulare e Molecolare “L. Califano,” Napoli, Italy; <sup>‡</sup>Istituto di Endocrinologia ed Oncologia Sperimentale del CNR, Università degli Studi di Napoli Federico II, Naples, Italy; <sup>§</sup>Dipartimento di Chimica, Università della Basilicata, Potenza, Italy

### Abstract

Activation of the Ras-Raf–extracellular signal–regulated kinase (ERK) pathway causes not only proliferation and suppression of apoptosis but also the antioncogenic response of senescence. How these contrasting effects are reconciled to achieve cell transformation and cancer formation is poorly understood. In a system of two-step carcinogenesis (dedifferentiated PC EIA, transformed PC EIA–polyoma–middle T [PC EIA + Py] and PC EIA–*v-raf* [PC EIA + raf] cells), *v-raf* cooperated with EIA by virtue of a strong prosurvival effect, not elicited by Py–middle T, evident toward serum-deprivation– and H<sub>2</sub>O<sub>2</sub>–induced apoptosis. Apoptosis was detected by DNA fragmentation and annexin V staining. The prosurvival function of *v-raf* was, in part, mitogen-activated protein kinase/ERK kinase (MEK)–dependent, as shown by pharmacological MEK inhibition. The MEK-dependent antiapoptotic effect of *v-raf* was exerted despite a lower level of P-ERK1/2 in EIA + raf cells with respect to EIA + Py/EIA cells, which was dependent on a high tyrosine phosphatase activity, as shown by orthovanadate blockade. An ERK1/2 tyrosine phosphatase was likely involved. The high tyrosine phosphatase activity was instrumental to the complete suppression of senescence, detected by β-galactosidase activity, because tyrosine phosphatase blockade induced senescence in EIA + raf but not in EIA + Py cells. High tyrosine phosphatase activity and evasion from senescence were confirmed in an anaplastic thyroid cancer cell line. Therefore, besides EIA, EIA + raf cells suppress senescence through a new mechanism, namely, phosphatase-mediated P-ERK1/2 inhibition, but, paradoxically, retain the oncogenic effects of the Raf-ERK pathway. We propose that the survival effect of Raf is not a function of absolute P-ERK1/2 levels at a given time but is rather dynamically dependent on greater variations after an apoptotic stimulus.

*Neoplasia* (2011) 13, 120–130

Abbreviations: ERK, extracellular signal–regulated kinase; MEK, mitogen-activated protein kinase/ERK kinase; MST2, mammalian sterile–twenty-like 2; MTT, (3-(4,5-dimethylthiazol-2-yl)-2,5-diphenol tetrazolium bromide; OA, okadaic acid; OIS, oncogene-induced senescence; OV, sodium orthovanadate; PC EIA, adenovirus EIA–transfected PC Cl3 cells; PC EIA + Py, adenovirus EIA–transfected, polyoma murine leukemia virus (carrying polyoma–middle T)–infected PC Cl3 cells; PC EIA + raf, adenovirus EIA–transfected, murine sarcoma virus 3611 (carrying *v-raf*)–infected PC Cl3 cells; SA-β-Gal, senescence-associated β-galactosidase

Address all correspondence to: Dr. Bruno Di Jeso, Dipartimento di Scienze e Tecnologie Biologiche ed Ambientali (DiSTeBA), Facoltà di Scienze Matematiche Fisiche e Naturali, Università degli Studi del Salento, Strada Provinciale Lecce-Monteroni, 73100 Lecce, Italy. E-mail: bruno.dijeso@unisalento.it

<sup>1</sup>This work was supported by MIUR (60% funds to B.D.J.). The authors declare no conflict of interest.

<sup>2</sup>This article refers to supplementary materials, which are designated by Figures W1 to W6 and are available online at [www.neoplasia.com](http://www.neoplasia.com).

<sup>3</sup>These authors contributed equally to this work.

Received 10 August 2010; Revised 12 November 2010; Accepted 18 November 2010

## Introduction

The Ras-Raf-extracellular signal-regulated kinase (ERK) pathway is frequently implicated in human cancers. Oncogenic mutations frequently occur in Ras and B-Raf, and ERK is frequently hyperactivated in human malignancies. Recently, mutations in C-Raf have been found in human cancers, located between the regulatory and kinase domains [1,2]. Raf kinase function has been analyzed well before the discovery of the mutations occurring in cancers because activated version of A-, B-, and C-Raf (including the retroviral version *v-raf*) were transforming for a variety of cell lines [3].

The mechanisms involved in Raf kinase transformation are stimulation of cell cycle progression and cell survival. Raf stimulates cell cycle progression mainly through transcriptional up-regulation of cyclin D1 and down-regulation of p27<sup>kip1</sup> [4]. Several mechanisms have been implicated in the survival activity of Raf. Described mechanisms require the kinase activity of Raf and mitogen-activated protein kinase/ERK kinase (MEK) [5,6], or the kinase activity of Raf, but in a MEK-independent manner. Thus, Raf activates, albeit indirectly, nuclear factor  $\kappa$ B (NF- $\kappa$ B) [7], it binds Bcl2 and BAG1 and is targeted to mitochondria where it exerts an antiapoptotic effect [8,9]. Finally, MEK-independent and Raf kinase-independent mechanisms have been reported. C-Raf binds to apoptosis signal regulating kinase (ASK1) and mammalian sterile-twenty-like 2 (MST2) and suppresses their proapoptotic activities in a kinase-independent manner [10,11]. Where tested, the MEK-independent/kinase-independent mechanisms are mediated by amino acids 151 to 303 of the regulatory N-terminus of C-Raf [11]. A MEK- and kinase-independent mechanism of the pro-survival function of Raf is also supported by *in vivo* data knocking in a kinase-dead mutant of C-Raf [12]. However, some controversies exist because the mutations used failed to completely inactivate Raf kinase activity [13–15]. Although true kinase-dead mutants of C-Raf were as efficient as wild-type Raf in interacting with MST2 and preventing apoptosis, this has been demonstrated only in tissue culture models [11]. In contrast, B-Raf V600E, that, *bona fide*, does not possess the MEK-independent and kinase-independent functions of C-Raf (the N-terminal domain of B-Raf is poorly homologous to that of C-Raf, and in fact, B-Raf does not bind MST2 [11]) suppresses apoptosis through an ERK-dependent BAD/BIM inactivation [16]. Therefore, the mechanism(s) of Raf antiapoptotic activity are still debated.

However, oncogenic activation of several components of the Ras-ERK pathway (Ras, C-Raf, B-Raf, MEK) induces cellular senescence (oncogene-induced senescence, OIS) [17–19]. This mechanism is operational *in vivo*, as demonstrated for murine lung adenomas, T-cell lymphomas, and benign melanocytic nevi [20–22].

Therefore, cancer cells exploit Raf activation for cell cycle progression and protection toward apoptosis, but this activation (and in general, an activation of the Ras-ERK pathway) may lead to OIS. Therefore, senescence must be bypassed to achieve a fully neoplastic phenotype. How this evasion is mediated is not completely understood. For example, melanomas, in addition to Ras/Raf mutations, frequently harbor inactivation of the *INK4 $\alpha$ /ARF* tumor suppressor locus, which inactivates the Rb (retinoblastoma) and p53 pathways [23]. However, it has been observed, in human nevi and in BRAF<sup>V600E</sup>-expressing melanocytes, a marked mosaic induction of p16<sup>INK4a</sup> [22]. This suggests that, in melanomas, mechanisms other than p16<sup>INK4a</sup> inactivation contribute to protection against B-Raf<sup>V600E</sup>-driven senescence. Thus, although a mosaic inactivation of p16<sup>INK4a</sup> could reflect the presence of senescent cells in the context of the tumor, it may be also indicative of additional mechanism bypassing OIS. However, the nature of these

additional mechanisms and if they are operative in other cytotypes is poorly understood.

In this study, we propose a new mechanism by which, at the same time, EIA + Raf-transformed cells completely suppress OIS through a phosphatase-mediated P-ERK1/2 inhibition, but, paradoxically, retain the oncogenic effects of Raf-ERK pathway activation such as protection from apoptosis, by a mechanism, at least in part, MEK-dependent.

## Materials and Methods

### Reagents and Antibodies

Sodium orthovanadate (OV), okadaic acid (OA), PD184352, and U0126 were from Calbiochem (La Jolla, CA). Anti-P-ERK Tyr 205/185 antibodies (sc-7383 able to detect P-Tyr 205/185 irrespective of the state of Thr 203/183) and anti-P-ERK P-Thr 203/183 antibodies (sc-101760 able to detect P-Thr 203/183 irrespective of the state of Tyr 205/185), anti-ERK2, anti-p16<sup>INK4a</sup>, anti-C-Raf, anti-I $\kappa$ B $\alpha$ , anti-Bcl2, anti-Bcl-XL, and anti-Bax antibodies were from Santa Cruz Biotechnologies (Santa Cruz, CA). Secondary horseradish peroxidase-conjugated antimouse and antirabbit antibodies were purchased from Amersham (Piscataway, NJ).

### Cell Culture

PC Cl3 cells were cultured in Coon modified Ham F-12 medium supplemented with 5% calf serum (GIBCO, Grand Island, NY), a six-hormone (6H) mixture as previously reported [24]. Dedifferentiated and transformed PC Cl3 cells (PC raf, PC Py, PC EIA, PC EIA + Py, and PC EIA + raf; a gift from Dr A. Fusco) were grown in the same medium lacking the 6H mixture. Anaplastic thyroid cancer FRO cells were a gift from Dr M. Santoro. These cells harbor the BRAF<sup>V600E</sup> mutation and are cultured in RPMI 1640 medium supplemented with 10% fetal bovine serum.

To induce growth factor deprivation, cells were starved for different times in a medium containing 0.2% BSA but lacking serum and hormones. Alternatively, cells were treated with H<sub>2</sub>O<sub>2</sub> at various concentrations, with daily additions of freshly prepared H<sub>2</sub>O<sub>2</sub>.

### Measurement of Apoptosis

Apoptosis was assessed by staining of cell membrane-exposed phosphatidylserine with fluorescein isothiocyanate-conjugated annexin V according to the manufacturer's description (Pharmingen, San Diego, CA). Samples were analyzed by flow cytometry using a FACSCalibur (Beckman Instruments, Fullerton, CA), equipped with ModFit Software. DNA fragmentation assay was performed as previously reported [25].

### MTT Assay and Western Blot

Cells at 70% to 80% confluence were trypsinized (0.25% trypsin with 1 mM EDTA), washed, resuspended in growth medium, and plated in 96-well plates with 0.1 ml of the 10<sup>4</sup> cell/ml cell suspension seeded in each well. After an overnight incubation, cells were treated with specific reagents for various times. The cell number was determined using a modified MTT (3-(4,5-dimethylthiazol-2-yl)-2,5-diphenol tetrazolium bromide) assay, as previously described [26]. The percentage of survival was calculated as the absorbance ratio of treated to untreated cells. The data presented are the mean  $\pm$  SD from eight replicate wells per microtiter plate and replicated four times. For Western blot assays, cells were treated with specific reagents (serum deprivation, H<sub>2</sub>O<sub>2</sub>, OV, OA) for various times. At the end of the treatments, cells were washed with

ice-cold phosphate-buffered saline (PBS) and harvested in Laemmli buffer (with  $\beta$ -mercaptoethanol) containing a mixture of phosphatase inhibitors (0.5 mM sodium vanadate, 2 mM sodium pyrophosphate, 5 mM  $\beta$ -glycerolphosphate, and 50 mM sodium fluoride) to prevent postlysis dephosphorylation. Western blots were carried out as previously reported [24].

### Senescence-Associated $\beta$ -Galactosidase

Cells were washed twice with PBS (pH 7.2), fixed with 0.5% glutaraldehyde in PBS, and washed in PBS supplemented with 1 mM  $MgCl_2$ . Cells were stained at room temperature in X-Gal solution

(1 mg/ml X-Gal, 0.12 mM  $K_3Fe[CN]_6$ , 0.12 mM  $K_4Fe[CN]_6$ , and 1 mM  $MgCl_2$  in PBS at pH 6.0). Staining was performed for 10 to 12 hours. Cells were washed in PBS three times and photographed with a Nikon AZ100 microscope equipped with a DS V1 camera (Nikon, Tokyo, Japan). For each condition, two replicate plates, of three different experiments, were examined. For each plate, staining was determined in four different microscope fields. The number of positively stained cells was estimated and expressed as the percentage of the total number of cells in the analyzed section. The microscopic fields were examined by two observers independently. Interobserver disagreement did not exceed 10% of the determined percent.

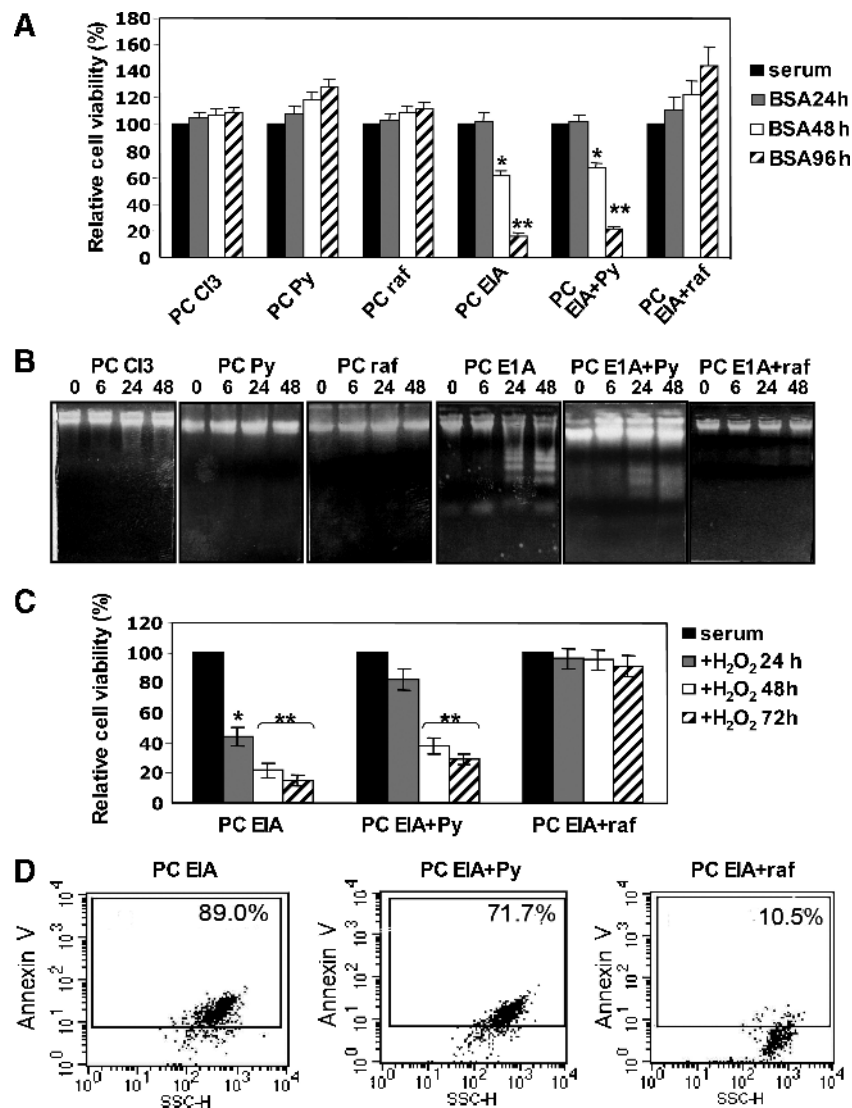


**Figure 1.** Transformed PC EIA + raf cells, but not transformed PC EIA + Py cells, are protected toward apoptosis triggered by growth factor deprivation or H<sub>2</sub>O<sub>2</sub>. (A, B) Normal, dedifferentiated, and transformed PC Cl3 cells were kept in the presence of serum (and hormones for normal PC Cl3 cells) or deprived of serum (and hormones for normal PC Cl3 cells), but in the presence of 0.2% BSA for 24, 48, and 96 hours (A) and for 6, 24, and 48 hours (B). At the end of the periods in serum-starved medium, cells were harvested and subjected to MTT assay (A) and DNA fragmentation assay (B) as outlined in Materials and Methods. In (A), the results shown are means  $\pm$  SD from eight replicate wells per microtiter plate of four different experiments. \* $P$  < .05, \*\* $P$  < .01, compared with untreated cells. (C, D) Dedifferentiated PC EIA and transformed PC EIA + Py and PC EIA + raf cells were exposed to daily additions of 400  $\mu$ M H<sub>2</sub>O<sub>2</sub> for 24, 48, and 72 hours (C) or for 48 hours (D). At the end of the treatments, cells were harvested and subjected to MTT assay (A) and annexin V staining (B) as outlined in Materials and Methods. In (A), the results shown are means  $\pm$  SD from eight replicate wells per microtiter plate of four different experiments. \* $P$  < .05, \*\* $P$  < .01, compared with untreated cells.

## Results

### Transformed PC EIA + raf Cells Are Protected toward Apoptosis whereas Transformed PC EIA + Py Cells Are Not

In this study, we used a system of two-step carcinogenesis. Normal cells are PC Cl3 cells, a differentiated rat thyroid epithelial cell line. The transfection of the adenovirus EIA gene was able to dedifferentiate PC Cl3 cells but was not able to transform them (PC EIA). A subsequent infection with PyMLV (carrying polyoma-middle T, PC EIA + Py cells) or MSV3611 (carrying *v-raf*, PC EIA + raf cells) conferred to PC EIA a high malignant phenotype. An infection of PC Cl3 with MSV3611 (PC raf cells) did not transform them, whereas an infection with PyMLV (PC Py cells) confers to PC Cl3 only a low tumorigenic phenotype. This system has been widely used because it reproduces a two-step carcinogenesis process in which the number and nature of the gene involved are known, although the mechanism underlying the cooperative effect of *v-raf* (and PyMT) with EIA was not defined. However, it was clear that EIA + raf cells were more tumorigenic than EIA + Py cells [27]. Because EIA confers to PC Cl3 a proliferation advantage [27], we seek to test whether PyMT and *v-raf* transform PC EIA cells through inhibition of apoptosis.

As shown in Figure 1A, growth factor deprivation did not modify cell viability of PC Cl3, PC raf, and PC Py cells, whereas it dramatically induced cell death in PC EIA and PC EIA + Py cells. However, PC EIA + raf cells were completely protected by growth factor deprivation-induced cell death. DNA fragmentation (Figure 1B) and propidium iodide staining (not shown) experiments indicated the occurrence of apoptotic cell death in EIA and EIA + Py cells. The marked apoptosis-suppressive effect of *v-raf* was present also with a different stimulus. Figure 1C shows that, after a daily addition of 400  $\mu$ M H<sub>2</sub>O<sub>2</sub>, there was a dramatic decrease in viability of EIA and EIA + Py cells, but again, the EIA + raf cells were protected toward cell death. H<sub>2</sub>O<sub>2</sub>-induced cell death was apoptotic, as shown by annexin V staining (Figure 1D).

### The *v-raf* Protective Effect Is, in Part, Mediated by Activation of Its Substrate MEK

Next, we seek to verify if the potent inhibitory effect of *v-raf* on apoptosis was mediated by *v-raf* kinase-dependent mechanism. This was reasonable because *v-raf*, lacking part of the N-terminal regulatory domain, may not be able to mediate the kinase- and MEK-independent effects on apoptosis [11].

As shown in Figure W1, EIA + raf cells express high levels of p79 gag-raf polypeptide and possibly low levels of p90 gag-raf polypeptide. The endogenous p72 C-Raf is likely under the detection limit of the antibodies (a similar differential expression, p79 > p90 > endogenous p72, has been reported [28]). Next, we explored ERK1/2 phosphorylation after apoptotic stimuli (Figure 2, A and B). In normal growth conditions, the analysis of the levels of P-ERK1/2 gave an unexpected result: despite the presence of a constitutively activated raf (Figure W1), EIA + raf cells displayed the lowest level of P-ERK1/2, approximately three times lower than EIA + Py cells, which showed the highest (Figures 2, 3, and 5). Growth factor deprivation caused a decrease in P-ERK1/2 in EIA and EIA + Py cells but not in EIA + raf cells (Figure 2A). After H<sub>2</sub>O<sub>2</sub> addition, EIA and EIA + Py cells showed a slight increase in P-ERK1/2 levels (~1.3-fold), whereas EIA + raf cells experienced a greater P-ERK1/2 induction (~2.5-fold; Figure 2B). However, even after serum deprivation and H<sub>2</sub>O<sub>2</sub>, the absolute levels of P-ERK1/2 in EIA + raf cells were not greater than those in EIA and EIA + Py cells.

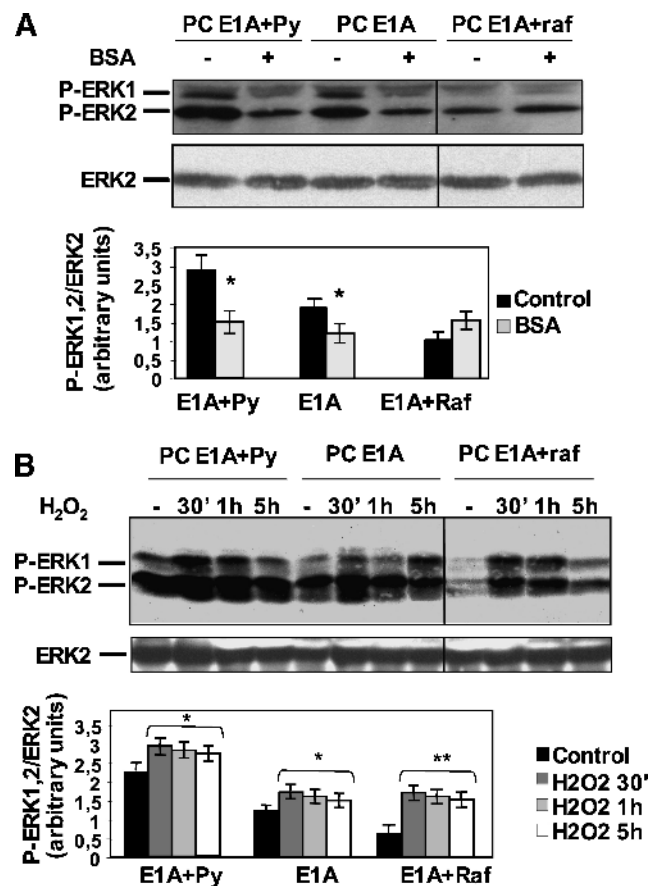


**Figure 2.** PC EIA + raf cells do not show a decrease in P-ERK1/2 after serum deprivation and show a greater induction in P-ERK1/2 after H<sub>2</sub>O<sub>2</sub> treatment with respect to PC EIA and PC EIA + Py cells. (A, B) Dedifferentiated PC EIA and transformed PC EIA + Py and PC EIA + raf cells were serum-starved (B) or exposed to 400  $\mu$ M H<sub>2</sub>O<sub>2</sub> (C) for the indicated times. Whole-cell lysates were prepared and immunoblotted using anti-P-ERK1/2 (anti-P-Tyr 205/185) or anti-ERK2 antibodies, as outlined in Materials and Methods. In (A) and (B), all lines were from the same blot. Mean values ( $\pm$ SD) of at least three independent experiments are shown. \* $P < .05$ , \*\* $P < .01$ , compared with untreated cells.

Because one mechanism of the prosurvival function of Raf is MEK-dependent [5,6], we seek to verify our intriguing findings (low absolute levels of P-ERK1/2, but high variations of P-ERK1/2 after an apoptotic stimulus in EIA + raf cells) with this possibility. Preliminarily, we determined the sensitivity of P-ERK1/2 levels to the specific MEK inhibitor PD184352. As shown in Figure 3, the effect of PD184352 was more evident in cells grown in serum (H<sub>2</sub>O<sub>2</sub> addition) than in cells grown in BSA. This is easily explained by (for example) different uptake rates of the drug in the two conditions. A greater efficacy of PD184352 in inhibiting the P-ERK levels in EIA + raf cells with respect to EIA + Py cells is also evident. From these experiments, we took the lowest concentrations of PD184352 able to nearly completely and to completely block ERK phosphorylation and measured cell survival after P-ERK1/2 blockade. Figure 4 shows that, in the presence of PD184352, EIA + raf cells significantly died in response to serum deprivation (Figure 4A) and to H<sub>2</sub>O<sub>2</sub> (Figure 4B). On the contrary, EIA + Py cells were insensitive to P-ERK1/2 blockade. However, a complete inhibition of P-ERK1/2 did not completely kill EIA + raf cells. Together, the results of Figures 2

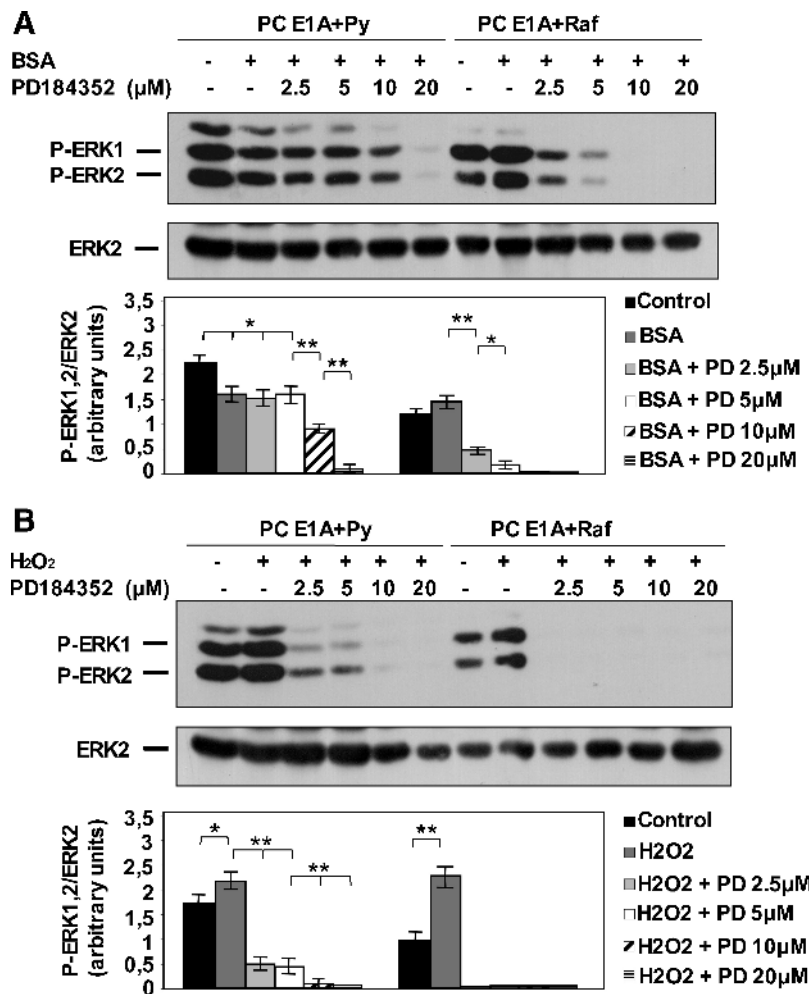


**Figure 3.** EIA + raf cells show a greater sensitivity with respect to EIA + Py cells to the MEK inhibitor PD184352. (A) PC EIA + Py and PC EIA + raf cells were mock-pretreated or pretreated with various concentrations of PD184352 for 30 minutes and then serum-starved for 3 days in the presence or absence of PD184352. (B) PC EIA + Py and PC EIA + raf cells were mock-pretreated or pretreated with various concentrations of PD184352 for 30 minutes and then exposed to 400  $\mu\text{M}$  H<sub>2</sub>O<sub>2</sub> for 30 minutes in the presence or absence of PD184352. After the treatments described in (A) and (B), whole-cell lysates were prepared and immunoblotted using anti-P-ERK1/2 (anti-P-Tyr 205/185) or anti-ERK2 antibodies, as outlined in Materials and Methods. The results shown are means  $\pm$  SD of at least three different experiments. \* $P < .05$ , \*\* $P < .01$ .

to 4 suggest that the antiapoptotic effect of *v-raf* is exerted, in part, through its substrate MEK1/2, and it is related more with the relative changes in ERK1/2 phosphorylation, after an apoptotic stimulus, than with their absolute levels.

Importantly, we did not find any effect of *v-raf* on the antiapoptotic NF- $\kappa$ B (whose activation by Raf is kinase-dependent but MEK-independent). EIA + raf cells showed higher levels of I $\kappa$ B $\alpha$  than EIA + Py cells, and after growth factor deprivation, both cell lines did not show any NF- $\kappa$ B activation (Figure W2A). We also found a surprisingly low level of Bcl2 in EIA + raf cells, lower than Bcl2 levels in PC EIA and PC EIA + Py cells, which did not change after growth factor deprivation (Figure W2B). This finding argues against a relevant antiapoptotic effect of *v-raf* mediated by Bcl2-dependent recruitment to mitochondria [8,9,29]. Moreover, the low levels of Bcl2 in PC EIA + raf cells were not balanced by high levels of Bcl-XL or by low levels of Bax, and their levels did not change after growth factor deprivation (Figure W2B).

Finally, these cell lines showed similar levels of intracellular ROS, which directly induced cell death and parallel slight variations of ROS

levels after growth factor deprivation (slight early increase and slow late decline; Figure W3).

#### *Low Levels of P-ERK1/2 in EIA + raf Cells Are Caused by a High Activity of Tyrosine Phosphatases*

Next, we sought to understand the mechanism that keeps levels of P-ERK1/2 low in EIA + raf cells. We hypothesized that phosphatase activity may be involved. Therefore, we treated EIA + Py and EIA + raf cells with the broad-spectrum Tyr and Ser/Thr phosphatase inhibitors OV and OA. As shown in Figure 5A, treatment with OV did not have a significant effect on the levels of P-ERK1/2 in EIA + Py cells, although it showed a dramatic effect in EIA + raf cells as detected by anti-Tyr 205/185 (murine ERK1/ERK2) antibodies (able to detect P-Tyr 205/185 irrespective of the state of Thr 203/183). As expected, no variation was detected by the same antibodies after OA treatment in both EIA + raf and EIA + Py cells (Figure W4A). To check the phosphorylation state of Thr 203/183, we used antibodies that detect P-Thr 203/183 irrespective of the state of Tyr 205/185. As shown

in Figure 5B, the P-Thr 203/183 levels were equal between EIA + Py and EIA + raf cells and did not change after OA treatment (also as expected, after OV treatment; Figure W4B). Thus, EIA + raf cells have an increased activity of tyrosine phosphatase(s) that decreased P-Tyr 205/185 in normal growth conditions.

Oxidative stress inhibits phosphatase activity [30], but H<sub>2</sub>O<sub>2</sub> and OV increased P-ERK1/2 in EIA + raf cells by 2- to 2.2- and 5- to 6-folds, respectively (Figure 2B vs Figure 5A). To understand this difference, we treated EIA + Py and EIA + raf cells with H<sub>2</sub>O<sub>2</sub> and OV separately and together. As shown in Figure 5C, OV was still able to increase, at the top of the H<sub>2</sub>O<sub>2</sub> effect, the levels of P-ERK1/2 in these cells, suggesting that the inhibitory effect of H<sub>2</sub>O<sub>2</sub> on phosphatase(s) was incomplete.

#### High Activity of Tyr Phosphatases in EIA + raf Cells Is Able to Prevent OIS

Because oncogenic activation of the Ras-ERK pathway is able to induce OIS, we reasoned that the high Tyr phosphatase activity of EIA + raf cells might contribute to avoid senescence, concurring to the high neoplastic phenotype of these cells.

To test this hypothesis, we first determined the effect of a Tyr phosphatase blockade on the growth of EIA + raf and EIA + Py cells. As shown in Figure 6A, EIA + raf cells dramatically slowed their growth rate (evaluated both by cell count and MTT assay) when treated with OV. In contrast, the growth of EIA + Py cells was insensitive to OV. Therefore, OV-increased P-ERK1/2 levels are paralleled by growth inhibition in EIA + raf cells, whereas EIA + Py cells show absence of OV effect both on P-ERK1/2 and on growth rate. Reciprocally, the lack of effect of OA on P-ERK1/2 levels in both EIA + raf and EIA + Py cells is reflected by no effect of OA on the growth of both cell lines (Figure 6A).

Moreover, most of the EIA + raf cells (~90%; Table 1) subjected to the Tyr phosphatase blockade showed an intense activity of senescence-associated  $\beta$ -galactosidase (SA- $\beta$ -Gal; Figure 6B), a marker for senescent or stressed cultured cells as well as for aged tissues *in vivo* [17]. Control EIA + raf cells (growth in normal condition) showed a negligible SA- $\beta$ -Gal activity (5%; Table 1). By contrast, control EIA + Py cells showed some SA- $\beta$ -Gal activity (~20%; Table 1), which was not increased on Tyr phosphatase blockade activity (Figure 6B and Table 1). Strikingly, the MEK-specific inhibitor PD184352 prevented the induction of SA- $\beta$ -Gal activity by OV in EIA + raf cells (Figure 6B and Table 1), establishing a causal link between P-ERK1/2 and SA- $\beta$ -Gal activity induction by OV. Moreover, OV stimulated the expression of p16<sup>INK4a</sup> in EIA + raf cells but not in EIA + Py cells (Figure 6C) and was unable to trigger apoptosis in EIA + raf cells (Figure 6D). These observations strongly strengthen the notion that OV is inducing cellular senescence in EIA + raf cells (Figure 6A–D).

These results indicate that, in EIA + raf cells, a high Tyr phosphatase activity contributes to completely suppress OIS that instead is present, at low levels, in control and Tyr phosphatase-inhibited EIA + Py cells.

Interestingly, a high Tyr phosphatase activity was confirmed in FRO anaplastic thyroid cancer cell line with the same approach used for EIA + raf cells. Thus, OV treatment increased approximately four-folds the P-ERK1/2 detected by anti-Tyr 205/185 (Figure 7A; and did not increase P-ERK1/2 detected by anti-Thr 203/183; Figure W6), whereas OA treatment did not increase P-ERK1/2 detected by both anti-Thr 203/183 (Figure 7B) and anti-Tyr 205/185 (Figure W6). Moreover, also in FRO cells, OV treatment dramatically slowed growth rate (Figure 7C) and caused an intense activity of SA- $\beta$ -Gal (Figure 7D).

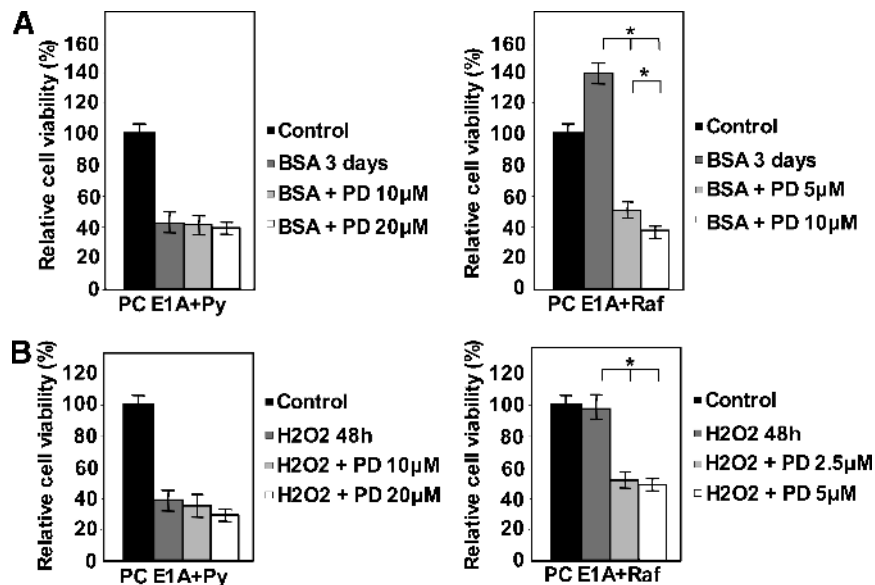


**Figure 4.** The MEK inhibitor PD184352 partly sensitizes EIA + raf but not EIA + Py cells toward apoptosis. (A) PC EIA + Py cells were mock-pretreated or pretreated with 10 and 20  $\mu$ M PD184352 for 30 minutes, whereas PC EIA + raf cells were mock-pretreated or pretreated with 5 and 10  $\mu$ M of PD184352 for 30 minutes. Cells were then serum-starved (with 0.2% BSA) for 3 days in the presence of PD184352. (B) PC EIA + Py cells were mock-pretreated or pretreated with 10 and 20  $\mu$ M of PD184352 for 30 minutes, whereas PC EIA + raf cells were mock-pretreated or pretreated with 2.5 and 5  $\mu$ M of PD184352 for 30 minutes. Cells were then exposed to 400  $\mu$ M H<sub>2</sub>O<sub>2</sub> for 48 hours in the presence of PD184352. After the treatments described in (A) and (B), cells were subjected to MTT assay, as outlined in Materials and Methods. The results shown are mean  $\pm$  SD from eight replicate wells per microtiter plate of four different experiments. \*\* $P < .01$ , compared with serum-deprived or H<sub>2</sub>O<sub>2</sub>-treated cells in the absence of PD184352.

## Discussion

In this study, we propose a new mechanism by which, in EIA + raf transformed cells, two effects, suppression of apoptosis and occurrence of OIS, linked by a high Raf activity, are uncoupled by virtue of increased Tyr phosphatase activity.

We used oncogene-transformed PC Cl3 cells that have been widely used to study multistep cancerogenesis [27]. However, the mechanisms underlying the cooperative effect of *v-raf* and PyMT with EIA have not been clearly defined, although it was clear that EIA + raf cells were more tumorigenic than EIA + Py cells [27]. Although PC EIA cells acquire a growth advantage with respect to PC Cl3 cells, they are not transformed [27], probably because they become highly susceptible to apoptosis (Figure 1). Therefore, PC EIA cells behave like several oncogene-expressing cells that become "sensitized" to various stresses [31]. The introduction of *v-raf* renders PC EIA cells completely resistant to apop-

toxis by the same stimuli (Figure 1), by a mechanism, in part, MEK-dependent (Figures 2–4). Reciprocally, EIA conceivably helps EIA + raf cells to bypass senescence by inactivating the Rb pathway. However, another mechanism is operational in EIA + raf cells to completely suppress senescence, as our data on Tyr phosphatase blockade indicate (see below). As a result, EIA + raf cells achieved a "resistant" state and are highly tumorigenic. We do not know exactly how PyMT transforms PC EIA cells. Probably, part of its action relies on a partial suppression of apoptosis, as we have seen when H<sub>2</sub>O<sub>2</sub> is applied (Figure 1). Thus, EIA + Py cells are reminiscent of cells in the "potentiated" state [32] that have only partly suppressed their "sensitized" state. Our results indicate that the "sensitized," "potentiated," and "resistant" states may be determined by the sequential activation of only two (and not necessarily three) oncogenes with the nature of the second determining if the "potentiated" or the "resistant" state is achieved.

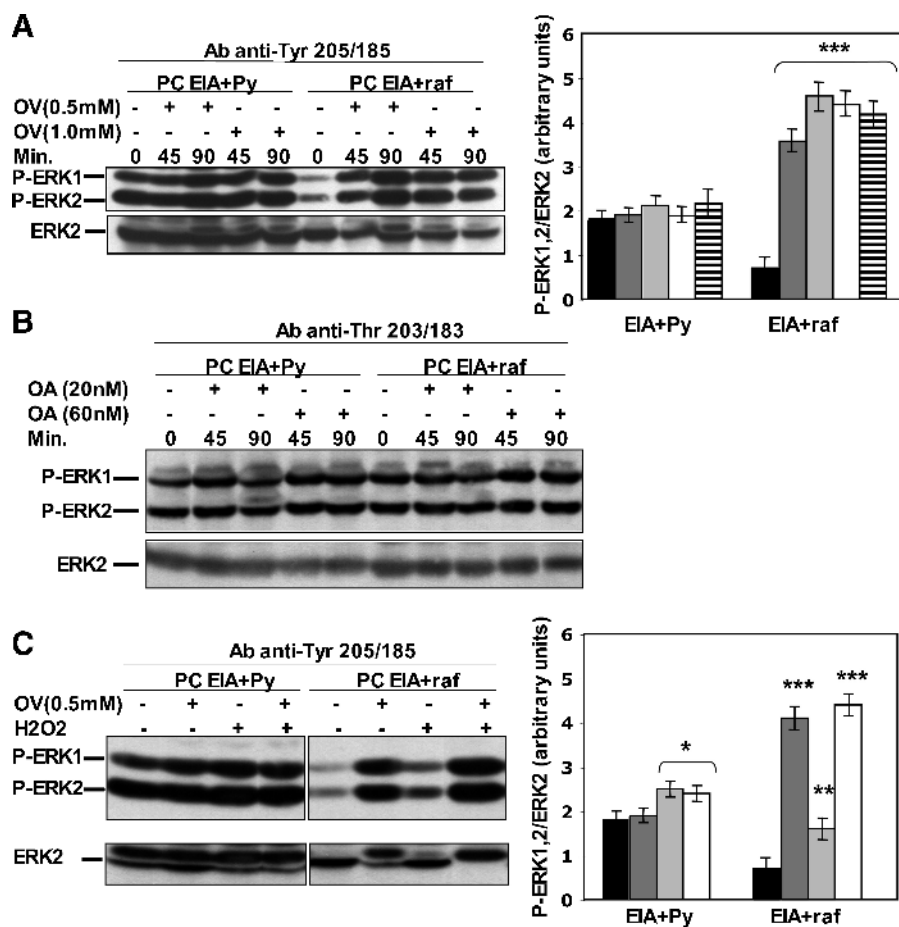


**Figure 5.** OV treatment increases Tyr 205/185 phosphorylation of ERK1/2 in EIA + raf but not in EIA + Py cells, whereas OA treatment does not increase Thr 203/183 phosphorylation neither in EIA + raf nor in EIA + Py cells. (A, B) Transformed PC EIA + Py and PC EIA + raf cells were treated with OV or OA for the indicated concentrations and times. Whole-cell lysates were prepared and immunoblotted using anti-P-ERK1/2 (anti-P-Tyr 205/185) antibodies (able to detect P-Tyr 205/185 irrespective of the state of Thr 203/183) (A) or anti-P-ERK1/2 (anti-Thr 203/183) antibodies (able to detect P-Thr 203/183 irrespective of the state of Tyr 205/185) (B) and anti-ERK2 antibodies (A and B) as outlined in Materials and Methods. The results shown are means  $\pm$  SD of at least three different experiments. \*\*\* $P$  < .001, compared with untreated cells. Black indicates control; dark gray, 0.5 mM OV 45 minutes; light gray, 0.5 mM OV 90 minutes; white, 1 mM OV 45 minutes; horizontal hatched, 1 mM OV 90 minutes. (C) Transformed PC EIA + Py and PC EIA + raf cells were treated with 0.5 mM OV or 400  $\mu$ M H<sub>2</sub>O<sub>2</sub> or 0.5 mM OV plus 400  $\mu$ M H<sub>2</sub>O<sub>2</sub> for 90 minutes. Whole-cell lysates were prepared and immunoblotted using anti-P-ERK1/2 (anti-Tyr 205/185) antibodies (able to detect P-Tyr 205/185 irrespective of the state of Thr 203/183) and anti-ERK2 antibodies as outlined in Materials and Methods. The results shown are means  $\pm$  SD of at least three different experiments. \* $P$  < .05, \*\* $P$  < .01, \*\*\* $P$  < .001, compared with untreated cells. Black indicates control; dark gray, 0.5 mM OV 45 minutes; light gray, 0.5 mM OV 90 minutes; white, 1 mM OV 45 minutes; horizontal hatched, 1 mM OV 90 minutes.

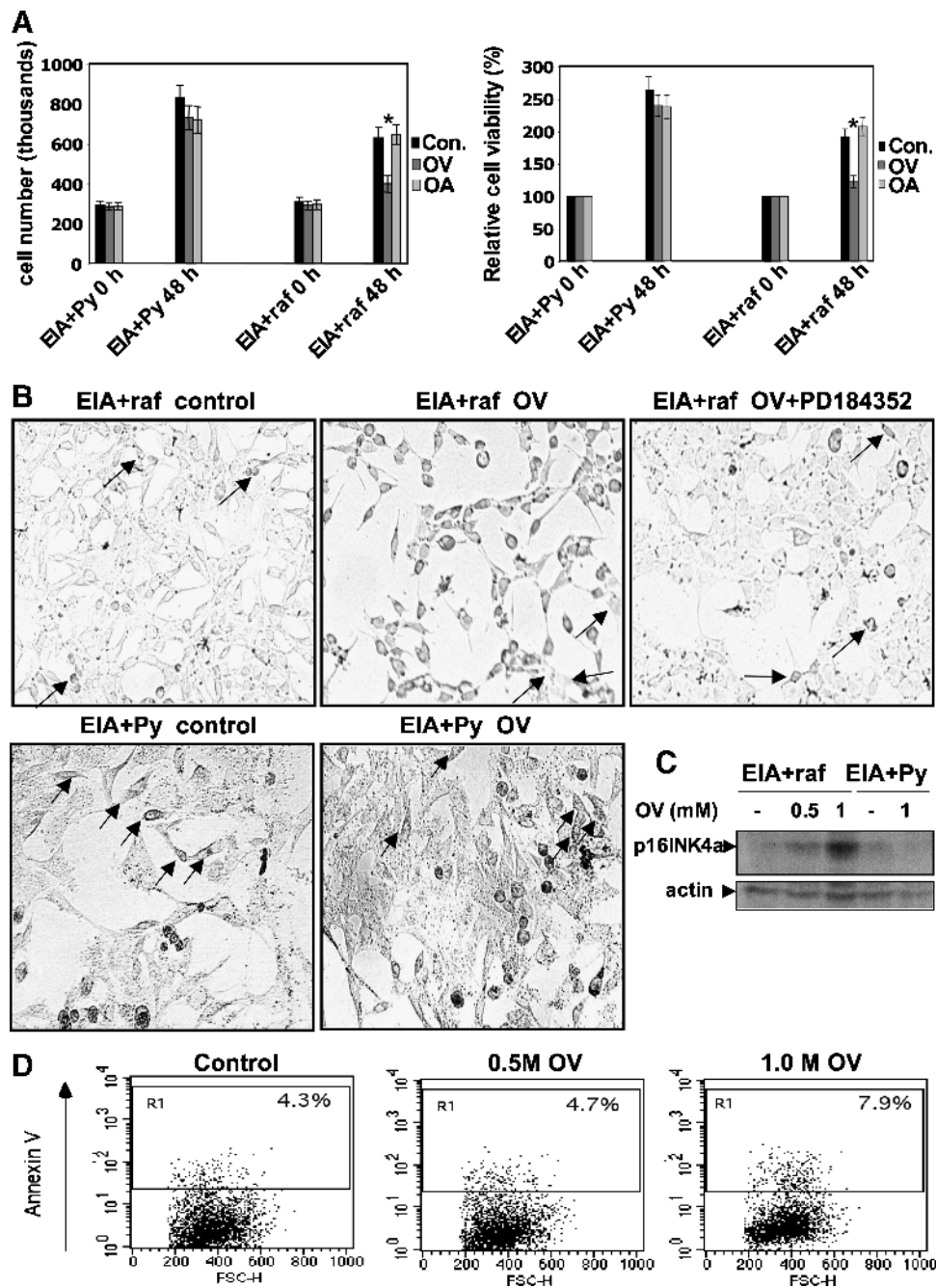


**Figure 6.** OV treatment causes the appearance of the hallmarks of senescence in EIA + raf but not in EIA + Py cells in the absence of apoptosis. (A) Transformed PC EIA + Py and PC EIA + raf cells were mock-treated (control) or treated with 0.5 mM OV or 60 nM OA for 90 minutes and then incubated with regular medium (without OV or OA) for 48 hours. Cells were counted and subjected to the MTT assay before starting the 90-minute OV/OA treatments and at the end of the 48-hour period in the regular medium without OV/OA. The results shown are means  $\pm$  SD from four plates (cell count) or eight replicate wells per microtiter plate (MTT assay) of four independent experiments. \* $P < .05$ , compared with untreated cells. (B) PC EIA + raf cells were mock-pretreated (control) or treated with 2.5  $\mu$ M PD184352, then mock-treated (control) or treated with 0.5 mM OV for 90 minutes and then incubated with regular medium (without OV) for 48 hours. PC EIA + Py cells were mock-treated (control) or treated with 0.5 mM OV for 90 minutes and then incubated with regular medium (without OV) for 48 hours. Control, OV-treated, and PD184352-pretreated–OV-treated cells were subjected to  $\beta$ -galactosidase staining at the end of the 48-hour period in the regular medium. In control and PD184352-pretreated–OV-treated EIA + raf cells, arrows indicate very few cells weakly stained with  $\beta$ -galactosidase; in OV-treated EIA + raf cells, arrows indicate few cells not stained with  $\beta$ -galactosidase. In control and OV-treated EIA + Py cells, arrows indicate several  $\beta$ -galactosidase–stained cells. (C) PC EIA + Py and PC EIA + raf cells were mock-treated (controls) or treated with 0.5 or 1 mM OV for 90 minutes and then incubated with regular medium (without OV or OA) for 48 hours. Whole-cell lysates were prepared and immunoblotted using anti-p16<sup>INK4a</sup> or antiactin antibodies, as outlined in Materials and Methods. The result shown is representative of at least three different experiments. (D) Transformed PC EIA + Py and PC EIA + raf cells were mock-treated (control) or treated with 0.5 or 1 mM OV for 90 minutes and then incubated with regular medium (without OV or OA) for 48 hours. Cells were subjected to annexin V staining at the end of the 48-hour period in the regular medium.



**Table 1.** Percent of SA- $\beta$ -Gal-Stained Cells.

	Control	OV	OV + PD184352
PC EIA + raf	6 $\pm$ 3	88 $\pm$ 7	9 $\pm$ 4
PC EIA + Py	18 $\pm$ 6	20 $\pm$ 8	—

The results shown are means  $\pm$  SD of two replicate plates of three different experiments. For each plate, staining was determined in four different microscope fields. The number of positively stained cells is expressed as the percentage of the total number of cells in the analyzed field. The microscopic fields were examined by two observers independently.

The mechanisms mediating the antiapoptotic activity of Raf are still debated. Described mechanisms require either the kinase activity of Raf and MEK or the kinase activity of Raf but not that of MEK (MEK-independent) or neither ones (MEK-independent/kinase-independent mechanisms) [5–12].

We have found that *v-raf* has a strong antiapoptotic effect. *v-raf* has a truncated N-terminus and may be unable or only partly able to elicit a MEK-independent and kinase-independent mechanism. In fact, *v-raf* should not bind MST2 because C-Raf binding to this kinase is

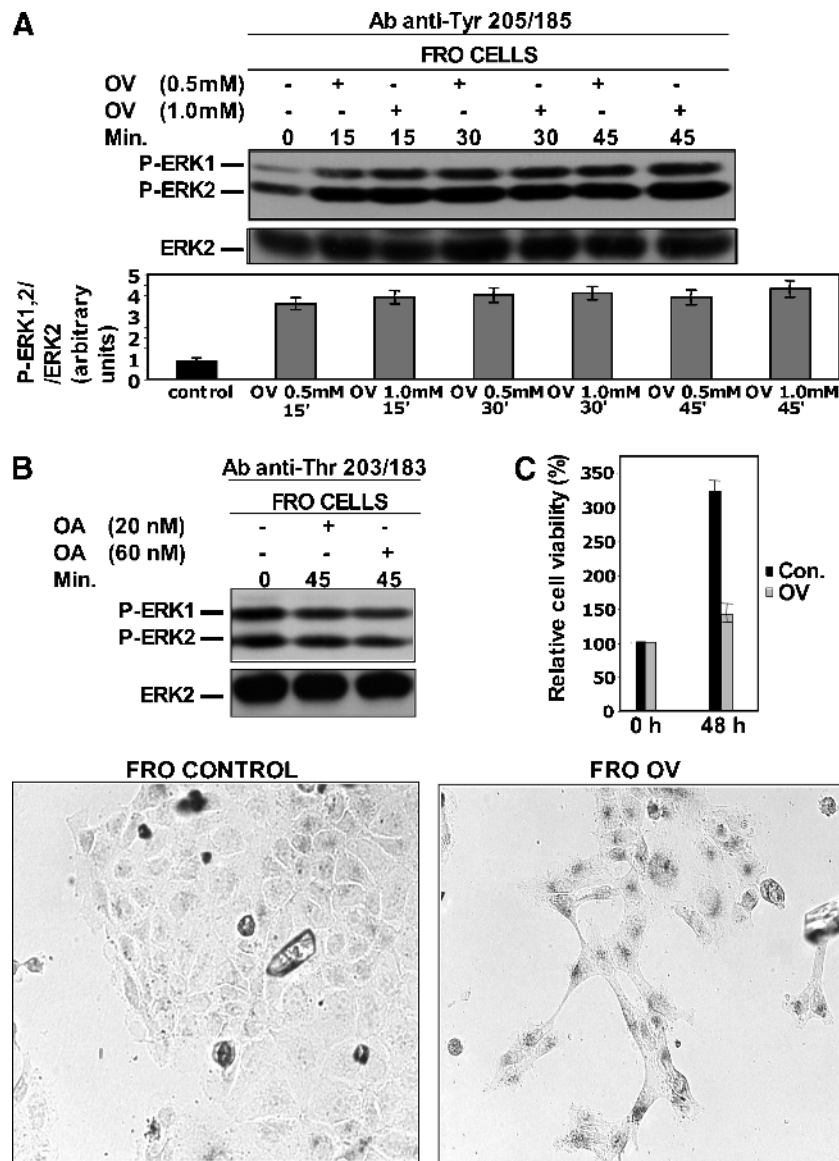


**Figure 7.** OV treatment increases Tyr 205/185 phosphorylation of ERK1/2 in FRO anaplastic thyroid cancer cells and causes the appearance of the hallmarks of senescence. (A, B) FRO cells were treated with OV or OA for the indicated concentrations and times. Whole-cell lysates were prepared and immunoblotted using anti-P-ERK1/2 (anti-P-Tyr 205/185) antibodies (able to detect P-Tyr 205/185 irrespective of the state of Thr 203/183) (A) or anti-P-ERK1/2 (anti-Thr 203/183) antibodies (able to detect P-Thr 203/183 irrespective of the state of Tyr 205/185) (B) and anti-ERK2 antibodies, as outlined in Materials and Methods. The results shown are means  $\pm$  SD of at least three different experiments. (C) FRO cells were mock-treated (control) or treated with 0.5 mM OV for 90 minutes and then incubated with regular medium (without OV) for 48 hours. Cells were subjected to the MTT assay before starting the 90-minute OV treatment and at the end of the 48-hour period in the regular medium without OV. The results shown are means  $\pm$  SD from eight replicate wells per microtiter plate of four independent experiments. (D) FRO cells were mock-treated (control) or treated with 0.5 mM OV for 90 minutes and then incubated with regular medium (without OV) for 48 hours. Control and OV-treated cells were subjected to  $\beta$ -galactosidase staining at the end of the 48-hour period in the regular medium.

mediated by amino acids 151 to 303 of the regulatory N-terminus of C-Raf [11]. *v-raf* should also be unable to elicit the survival effect mediated by its interaction with ASK-1. Two recent observations support this hypothesis. C-Raf protects endothelial cells by genotoxic stress by inhibiting ASK-1 at mitochondria [33] and the N-terminus of C-Raf mediates its interaction with mitochondria as the 323 to 648 C-terminus (coincident with *v-raf*) is unable to interact with mitochondria [34].

Accordingly with these considerations, we have found that the pro-survival effect of *v-raf* is, in part, MEK-dependent (Figure 4). However, surprisingly, the P-ERK1/2 levels of EIA + raf cells, in normal serum (Figures 2, 3, and 5), and after the application of the apoptotic stimulus (Figures 2 and 3) were not greater with respect to the EIA + Py cells. Thus, these results configure a paradox: how can lower levels of P-ERK1/2 be protective toward apoptosis by a MEK-dependent mechanism, whereas higher levels cannot? We observed that apoptosis resistance of EIA + raf cells correlated more with a higher dynamic range of P-ERK1/2 after the apoptotic stimulus than with their absolute levels (Figure 2).

The low levels of P-ERK1/2 in EIA + raf cells struck us. We reasoned that they might reflect the presence of adaptation mechanisms like increased phosphatase activity in the Ras-ERK pathway [35,36]. Indeed, treatments with the general Tyr phosphatase inhibitor OV dramatically increased the levels of P-ERK1/2 in EIA + raf but not in EIA + Py cells. On the contrary, the Ser/Thr phosphatase inhibitor OA did not increase P-ERK1/2 levels neither in EIA + raf nor in EIA + Py cells. Therefore, EIA + raf but not EIA + Py cells have developed a high Tyr phosphatase activity that keeps a low level of P-ERK1/2 in the face of constitutive Raf activation.

Of note, at least some of our observations of the greater dynamic range of P-ERK1/2 after apoptotic stimuli are explained by the higher phosphatase activity of EIA + raf cells. Thus, P-ERK1/2 induction by H<sub>2</sub>O<sub>2</sub> (Figure 2B) is likely the result of Tyr phosphatase inhibition (because ROS inactivates Tyr phosphatase [30]). Therefore, EIA + raf cells, which have a greater phosphatase activity, experience a greater P-ERK1/2 induction after inhibition. Furthermore, the effect of serum deprivation in EIA + raf cells (Figure 2A) may partly contribute to Tyr phosphatase inhibition by ROS, which transiently increases in this condition (Figure W3).

Interestingly, we found that EIA + raf cells were more sensitive than EIA + Py cells to the inhibitory action of PD184352 (Figure 3). We do not know the reason of this differential sensitivity, but it might represent an additional factor contributing to the effectiveness of PD184352 in decreasing the survival of EIA + raf cells.

As far as the nature of the phosphatase(s) involved is concerned, it is unlikely that a Raf phosphatase [37] or a dual-specificity phosphatase (DUSP) [35,38] is involved. In fact, our data suggest that ERK1/2 in EIA + raf cells is selectively dephosphorylated in Tyr 205/185. If a Raf-Tyr phosphatase or a DUSP was, in fact, involved, an increase in both P-Tyr 205/185 and P-Thr 203/183 of ERK was expected after inhibition. The differential phosphorylation of Tyr and Thr of the activation loop suggests that a Tyr phosphatase acting on ERK1/2 is involved. Increased expression of several Tyr phosphatases, including some considered tumor suppressors, has been reported in a variety of tumors [39], and ERK1/2 is increasingly demonstrated as a Tyr phosphatase substrate [40].

In EIA + raf cells, the phosphatase-mediated P-ERK1/2 inhibition affects cellular senescence. The EIA gene has a senescence-inhibiting effect by inactivating the Rb pathway [41], and this mechanism should

operate in EIA + raf cells. However, in these cells, a high Tyr phosphatase activity allows a complete suppression of OIS. Thus, on Tyr phosphatase inhibition and subsequent increase in P-ERK1/2, EIA + raf cells undergo OIS in the presence of EIA. P-ERK1/2 induction was causally linked to induction of senescence as shown by the inhibition of induction of senescence by the MEK inhibitor PD184352 (Figure 6). Analogously, in EIA + Py cells, EIA inhibits senescence. However, they show a low degree of senescence (absent in EIA + raf cells; Figures 6 and W5), which does not increase on Tyr phosphatase inhibition, probably linked to the absence of Tyr phosphatase activity and to the higher P-ERK1/2 levels with respect to EIA + raf cells.

Therefore, it seems that a high phosphatase activity and, consequently, low P-ERK1/2 levels are exploited to completely suppress senescence, a goal not achieved when phosphatase activity is low and P-ERK1/2 levels are higher. This is a proximal mechanism to bypass senescence, directly opposing, at the posttranslational level, the abrupt oncogene-induced ERK stimulation. It is at variance with distal mechanisms opposing the Rb and p53 pathways such as inactivation of the *INK4a/ARF* locus [23].

Strikingly, in EIA + raf cells, the phosphatase-mediated P-ERK1/2 inhibition, instrumental to bypass senescence, paradoxically coexists with a MEK-dependent protection from apoptosis, as pointed out before. We propose that the survival effect of *raf* is not a function of absolute P-ERK1/2 levels at a given time but, rather, is dynamically dependent on greater variations after an apoptotic stimulus. It may seem contradictory that positive variations of P-ERK1/2 both protect toward apoptosis and trigger senescence. This may rely on the different dynamic ranges of P-ERK1/2 induction: absence of diminution (serum deprivation) or 2- to 2.5-folds induction (H<sub>2</sub>O<sub>2</sub> treatment) protect toward apoptosis, whereas 5- to 6-folds induction triggers senescence (directly compared in Figure 5C).

The lack of correlation described here between the expression of constitutively activated Raf and P-ERK is reminiscent of what has been found in some human tumors. Thus, ERK1/2 activation does not correlate with K-Ras and B-Raf status in endometrial cancers [42], with N-Ras and B-Raf status in melanomas [43], and with the B-Raf status in papillary thyroid carcinoma [44]. In some cases, even a paradoxical correlation between low P-ERK1/2 levels and adverse prognosis has been found [42,45,46]. The results presented here may help to interpret these poorly understood *in vivo* observations and to identify new therapeutic targets in the actively investigated Tyr phosphatase family.

## Acknowledgments

The authors thank Alfredo Fusco for the PC system of transformed thyroid cells and for stimulating our interest in thyroid cancerogenesis.

## References

- Emuss V, Garnett M, Mason C, and Marais R (2005). Mutations of C-RAF are rare in human cancer because C-RAF has a low basal kinase activity compared with B-RAF. *Cancer Res* **65**, 9719–9726.
- Zebisch A, Staber PB, Delavar A, Bodner C, Hiden K, Fischereder K, Janakiraman M, Linkesch W, Auner HW, Emberger W, et al. (2006). Two transforming C-RAF germ-line mutations identified in patients with therapy-related acute myeloid leukemia. *Cancer Res* **66**, 3401–3408.
- Daum G, Eisenmann-Tappe I, Fries HW, Troppmair J, and Rapp UR (1994). The ins and outs of Raf kinases. *Trends Biochem Sci* **19**, 474–480.
- Kerkhoff E and Rapp UR (1998). Cell cycle targets of Ras/Raf signalling. *Oncogene* **17**, 1457–1462.
- Weston CR, Balmanno K, Chalmers C, Hadfield K, Molton SA, Ley R, Wagner EF, and Cook SJ (2003). Activation of ERK1/2 by deltaRaf-1:ER\* represses Bim expression independently of the JNK or PI3K pathways. *Oncogene* **22**, 1281–1293.

- [6] von Gise A, Lorenz P, Wellbrock C, Hemmings B, Berberich-Siebelt F, Rapp UR, and Troppmair J (2001). Apoptosis suppression by Raf-1 and MEK1 requires MEK- and phosphatidylinositol 3-kinase-dependent signals. *Mol Cell Biol* **21**, 2324–2336.
- [7] Baumann B, Weber CK, Troppmair J, Whiteside S, Israel A, and Rapp UR (2000). Raf induces NF- $\kappa$ B by membrane shuttle kinase MEK1, a signaling pathway critical for transformation. *Proc Natl Acad Sci USA* **97**, 4615–4620.
- [8] Wang HG, Rapp UR, and Reed JC (1996a). Bcl-2 targets the protein kinase Raf-1 to mitochondria. *Cell* **87**, 629–638.
- [9] Wang HG, Takayama S, Rapp UR, and Reed JC (1996b). Bcl-2 interacting protein, BAG-1, binds to and activates the kinase Raf-1. *Proc Natl Acad Sci USA* **93**, 7063–7068.
- [10] Chen J, Fujii K, Zhang L, Roberts T, and Fu H (2001). Raf-1 promotes cell survival by antagonizing apoptosis signal-regulating kinase 1 through a MEK-ERK independent mechanism. *Proc Natl Acad Sci USA* **98**, 7783–7788.
- [11] O'Neill E, Rushworth L, Baccharini M, and Kolch W (2004). Role of the kinase MST2 in suppression of apoptosis by the proto-oncogene product Raf-1. *Science* **306**, 2267–2270.
- [12] Hüser M, Luckett J, Chiloeches A, Mercer K, Iwobi M, Giblett S, Sun XM, Brown J, Marais R, and Pritchard C (2001). MEK kinase activity is not necessary for Raf-1 function. *EMBO J* **20**, 1940–1951.
- [13] Fabian JR, Daar IO, and Morrison DK (1993). Critical tyrosine residues regulate the enzymatic and biological activity of Raf-1 kinase. *Mol Cell Biol* **13**, 7170–7179.
- [14] Bosch E, Cherwinski H, Peterson D, and McMahon M (1997). Mutations of critical amino acids affect the biological and biochemical properties of oncogenic A-Raf and Raf-1. *Oncogene* **15**, 1021–1033.
- [15] Barnard D, Diaz B, Clawson D, and Marshall M (1998). Oncogenes, growth factors and phorbol esters regulate Raf-1 through common mechanisms. *Oncogene* **17**, 1539–1547.
- [16] Sheridan C, Brumatti G, and Martin SJ (2008). Oncogenic B-Raf<sup>V600E</sup> inhibits apoptosis and promotes ERK-dependent inactivation of Bad and Bim. *J Biol Chem* **283**, 22128–22135.
- [17] Serrano M, Lin AW, McCurrach ME, Beach D, and Lowe SW (1997). Oncogenic *ras* provokes premature cell senescence associated with accumulation of p53 and p16<sup>INK4a</sup>. *Cell* **88**, 593–602.
- [18] Zhu J, Woods D, McMahon M, and Bishop JM (1998). Senescence of human fibroblasts induced by oncogenic Raf. *Genes Dev* **12**, 2997–3007.
- [19] Lin AW, Barradas M, Stone JC, van Aelst L, Serrano M, and Lowe SW (1998). Premature senescence involving p53 and p16 is activated in response to constitutive MEK/MAPK mitogenic signaling. *Genes Dev* **12**, 3008–3019.
- [20] Collado M, Gil J, Efeyan A, Guerra C, Schuhmacher AJ, Barradas M, Benguría A, Zaballos A, Flores JM, Barbacid M, et al. (2005). Tumour biology: senescence in premalignant tumours. *Nature* **436**, 642.
- [21] Braig M, Lee S, Loddenkemper C, Rudolph C, Peters AH, Schlegelberger B, Stein H, Dörken B, Jenuwein T, and Schmitt CA (2005). Oncogene-induced senescence as an initial barrier in lymphoma development. *Nature* **436**, 660–665.
- [22] Michaloglou C, Vredeveld LC, Soengas MS, Denoyelle C, Kuilman T, van der Horst CM, Majoor DM, Shay JW, Mooi WJ, and Peepers DS (2005). BRAF<sup>E600</sup>-associated senescence-like cell cycle arrest of human naevi. *Nature* **436**, 720–724.
- [23] Curtin JA, Fridlyand J, Kageshita T, Patel HN, Busam KJ, Kutzner H, Cho KH, Aiba S, Bröcker EB, LeBoit PE, et al. (2005). Distinct sets of genetic alterations in melanoma. *N Engl J Med* **353**, 2135–2147.
- [24] Di Jeso B, Park YN, Ulianich L, Treglia AS, Urbanas ML, High S, and Arvan P (2005). Mixed-disulfide folding intermediates between thyroglobulin and endoplasmic reticulum resident oxidoreductases ERp57 and protein disulfide isomerase. *Mol Cell Biol* **25**, 9793–9805.
- [25] Di Jeso B, Ulianich L, Racioppi L, D'Armiento F, Feliciello A, Pacifico F, Consiglio E, and Formisano S (1995). Serum withdrawal induces apoptotic cell death in Ki-*ras* transformed but not in normal differentiated thyroid cells. *Biochem Biophys Res Commun* **214**, 819–824.
- [26] Mosmann T (1993). Rapid colorimetric assay for cellular growth and survival: application to proliferation and cytotoxicity assay. *J Immunol Methods* **65**, 55–63.
- [27] Berlingieri MT, Santoro M, Battaglia C, Grieco M, and Fusco A (1993). The adenovirus E1A gene blocks the differentiation of a thyroid epithelial cell line, however the neoplastic phenotype is achieved only after cooperation with other oncogenes. *Oncogene* **8**, 249–255.
- [28] Huleihel M, Goldsborough LM, Cleveland J, Gunnell M, Bonner T, and Rapp UR (1986). Characterization of murine A-*raf*, a new oncogene related to the v-*raf* oncogene. *Mol Cell Biol* **6**, 2655–2662.
- [29] Jin S, Zhuo Y, Guo W, and Field J (2005). p21-activated kinase 1 (Pak1)-dependent phosphorylation of Raf-1 regulates its mitochondrial localization, phosphorylation of BAD, and Bcl-2 association. *J Biol Chem* **280**, 24698–24705.
- [30] den Hertog J, Ostman A, and Böhmer FD (2008). Protein tyrosine phosphatases: regulatory mechanisms. *FEBS J* **275**, 831–847.
- [31] Evan GI and Vousden KH (2001). Proliferation, cell cycle and apoptosis in cancer. *Nature* **411**, 342–348.
- [32] Benhar M, Engelberg D, and Levitzki A (2002). ROS, stress-activated kinases and stress signaling in cancer. *EMBO Rep* **3**, 420–425.
- [33] Alavi AS, Acevedo L, Min W, and Cheresch DA (2007). Chemoresistance of endothelial cells induced by basic fibroblast growth factor depends on Raf-1-mediated inhibition of the proapoptotic kinase, ASK1. *Cancer Res* **67**, 2766–2772.
- [34] Galmiche A, Fueller J, Santel A, Krohne G, Wittig I, Doye A, Rolando M, Flatau G, Lemichez E, and Rapp UR (2008). Isoform-specific interaction of C-RAF with mitochondria. *J Biol Chem* **283**, 14857–14866.
- [35] Keyse SM (2008). Dual-specificity MAP kinase phosphatases (MKPs) and cancer. *Cancer Metastasis Rev* **27**, 253–261.
- [36] Saxena M and Mustelin T (2000). Extracellular signals and scores of phosphatases: all roads lead to MAP kinase. *Semin Immunol* **12**, 387–396.
- [37] Dhillon AS, von Kriegsheim A, Grindlay J, and Kolch W (2007). Phosphatase and feedback regulation of Raf-1 signaling. *Cell Cycle* **6**, 3–7.
- [38] Tonks NK (2006). Protein tyrosine phosphatases: from genes, to function, to disease. *Nat Rev Mol Cell Biol* **7**, 833–846.
- [39] Ostman A, Hellberg C, and Böhmer FD (2006). Protein-tyrosine phosphatases and cancer. *Nat Rev Cancer* **6**, 307–320.
- [40] Sacco F, Tinti M, Palma A, Ferrari E, Nardoza AP, Hooft van Huijsduijnen R, Takahashi T, Castagnoli L, and Cesareni G (2009). Tumor suppressor density-enhanced phosphatase-1 (DEP-1) inhibits the RAS pathway by direct dephosphorylation of ERK1/2 kinases. *J Biol Chem* **284**, 22048–22058.
- [41] O'Shea CC (2005). DNA tumor viruses—the spies who lyse us. *Curr Opin Genet Dev* **15**, 18–26.
- [42] Mizumoto Y, Kyo S, Mori N, Sakaguchi J, Ohno S, Maida Y, Hashimoto M, Takakura M, and Inoue M (2007). Activation of ERK1/2 occurs independently of KRAS or BRAF status in endometrial cancer and is associated with favorable prognosis. *Cancer Sci* **98**, 652–658.
- [43] Houben R, Vetter-Kauczok CS, Ortman S, Rapp UR, Broecker EB, and Becker JC (2008). Phospho-ERK staining is a poor indicator of the mutational status of BRAF and NRAS in human melanoma. *J Invest Dermatol* **128**, 2003–2012.
- [44] Zuo H, Nakamura Y, Yasuoka H, Zhang P, Nakamura M, Mori I, Miyauchi A, and Kakudo K (2007). Lack of association between BRAF V600E mutation and mitogen-activated protein kinase activation in papillary thyroid carcinoma. *Pathol Int* **57**, 12–20.
- [45] Jovanovic B, Kröckel D, Linden D, Nilsson B, Eghyazi S, and Hansson J (2008). Lack of cytoplasmic ERK activation is an independent adverse prognostic factor in primary cutaneous melanoma. *J Invest Dermatol* **128**, 2696–2704.
- [46] Lee HJ, Kim DI, Kang GH, Kwak C, Ku JH, and Moon KC (2009). Phosphorylation of ERK1/2 and prognosis of clear cell renal cell carcinoma. *Urology* **73**, 394–399.

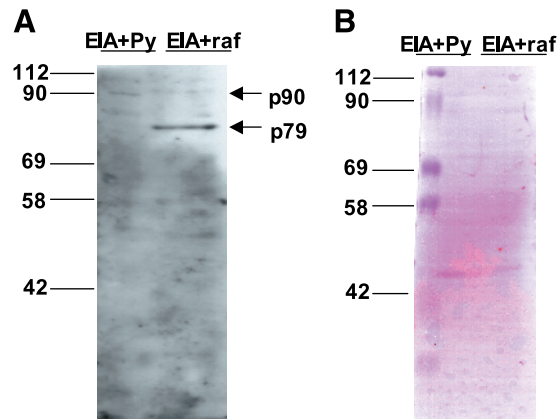


**Figure W1.** EIA + raf cells express a high level of p79 gag-raf polyprotein. PC EIA + Py and PC EIA + raf cells, grown in normal conditions (5% calf serum), were harvested, and whole-cell lysates were immunoblotted with anti-C-Raf antibodies (A). For control of loading, the filter was stained with Ponceau S (B).

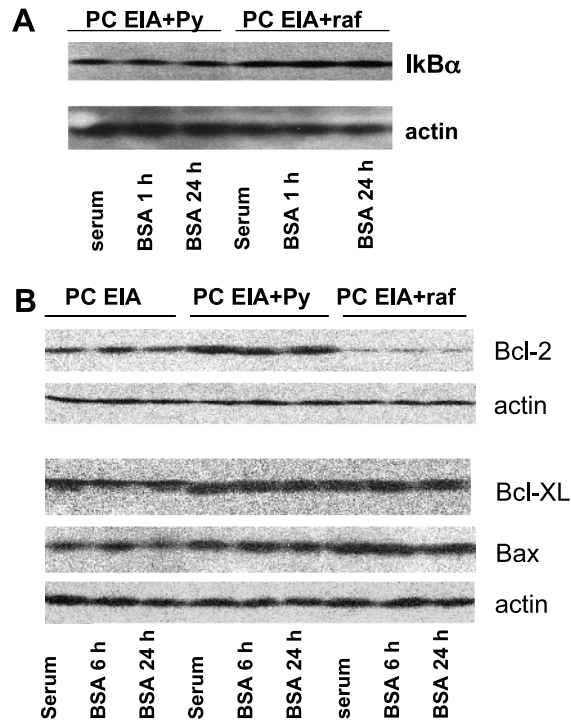


**Figure W2.** NF- $\kappa$ B is not activated in EIA + raf and EIA + Py cells after growth factor deprivation. EIA + raf cells show lower levels of Bcl2 and equal levels of Bcl-XL and Bax with respect to EIA + Py cells. Cells were kept in the presence of serum or deprived of serum in the presence of 0.2% BSA for 48 hours. At the end of this period in the serum-starved medium, cells were harvested. Whole-cell lysates were prepared and immunoblotted using anti-I $\kappa$ B $\alpha$ , anti-Bcl2, anti-Bcl-XL, and anti-Bax antibodies as outlined in Materials and Methods.

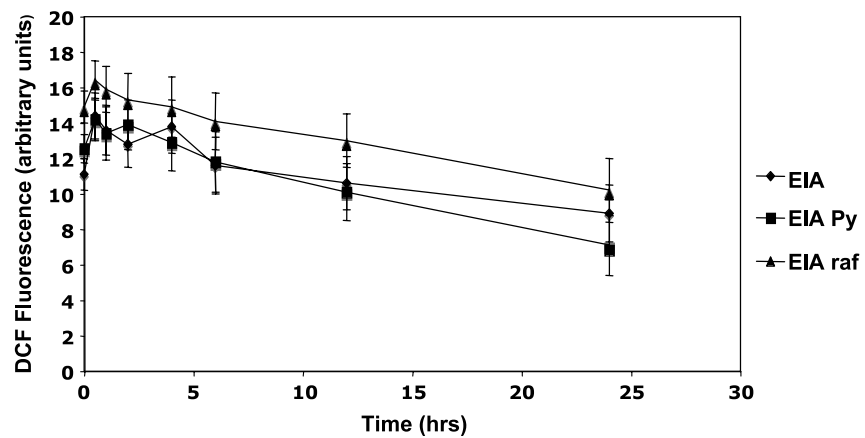


**Figure W3.** Estimation of intracellular ROS level. Cells were kept in the presence of serum or deprived of serum in the presence of 0.2% BSA for various periods. Floating and adherent cells were collected by mild trypsinization, washed in PBS, and resuspended in PBS, 10  $\mu$ M 5,6-carboxy-2',7'-dichlorofluorescein diacetate (DCFH-DA; Molecular Probes, Inc, Eugene, OR), 5  $\mu$ g/ml propidium iodide at 37°C, and kept in DCFH-DA thereafter. DCFH-DA is a compound taken up by the cells and trapped in a nonfluorescent deacylated form (DCFH). DCFH is oxidized by ROS to a fluorescent form. After 1 hour of incubation, cells were analyzed by FACScan with excitation at 495-nm and emission at 525-nm wavelengths. Nonintact cells leak DCFH but were stained by propidium iodide and excluded. The results shown are means  $\pm$  SD of at least three different experiments.

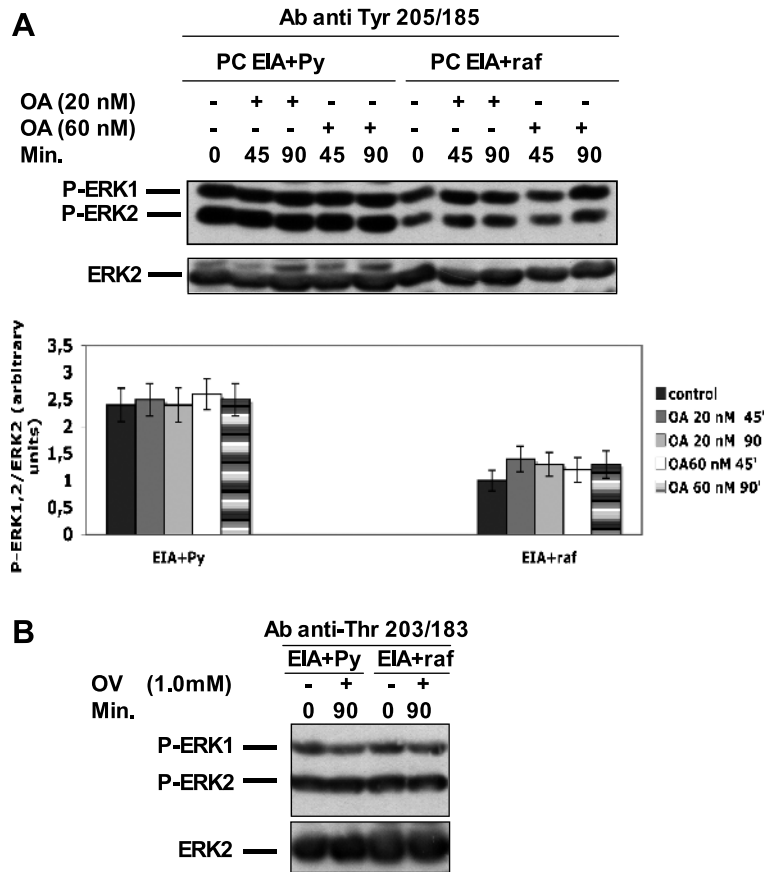


**Figure W4.** OA treatment does not increase Tyr 205/185 phosphorylation, and OV treatment does not increase Thr 203/183 phosphorylation neither in EIA + raf nor in EIA+Py cells. EIA + raf and EIA+Py cells were treated with OA (A) or OV (B) for the indicated concentrations and times. Whole cell lysates were prepared and immunoblotted using anti-P-ERK1/2 (anti-P-Tyr 205/185 antibodies, able to detect P-Tyr 205/185 irrespective of the state of Thr 203/183) (A) and anti-P-ERK1/2 (anti-Thr 203/183 antibodies, able to detect P-Thr 203/183 irrespective of the state of Tyr 205/185) (B), and anti-ERK2 antibodies, as outlined in Materials and Methods. In (A), the results shown are means  $\pm$  SD of three independent experiments. In (B), a representative experiment of three independent experiments is shown.

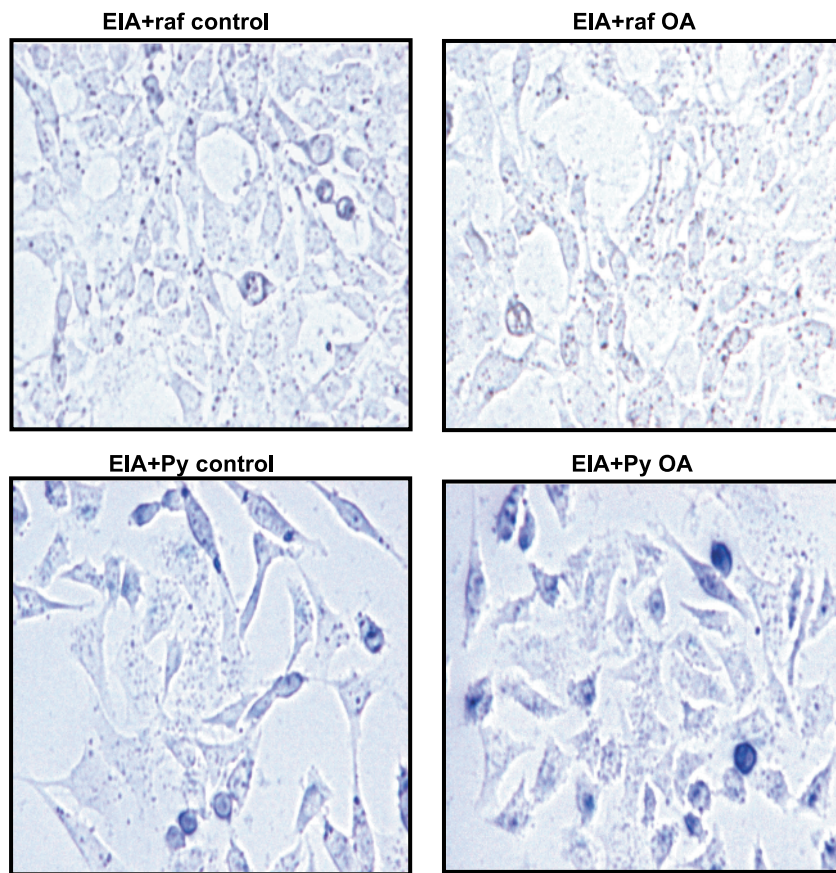


**Figure W5.** OA treatment does not cause the appearance of the hallmarks of senescence in both EIA + raf and EIA + Py cells. Transformed PC EIA + raf and PC EIA+Py cells were mock-treated or treated with 60 nM OA for 90 minutes and then incubated with regular medium (without OA) for 48 hours. Control and OA-treated cells were subjected to  $\beta$ -galactosidase staining at the end of the 48-hour period in the regular medium without OA.

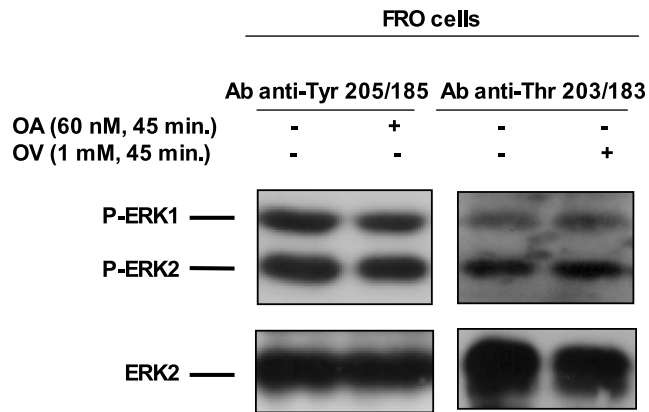


**Figure W6.** OA treatment does not increase Tyr 205/185 phosphorylation, and OV treatment does not increase Thr 203/183 phosphorylation in FRO anaplastic thyroid cancer cells. FRO cells were treated with OA or OV for the indicated concentrations and times. Whole-cell lysates were prepared and immunoblotted using anti-P-ERK1/2 (anti-P-Tyr 205/185 antibodies, able to detect P-Tyr 205/185 irrespective of the state of Thr 203/183) and anti-P-ERK1/2 (anti-Thr 203/183 antibodies, able to detect P-Thr 203/183 irrespective of the state of Tyr 205/185) and anti-ERK2 antibodies, as outlined in Materials and Methods. A representative experiment of three independent experiments is shown.